© 3rd IAHR Europe Congress, Book of Proceedings, 2014, Porto - Portugal. ISBN 978-989-96479-2-3

FAILURE BY OVERTOPPING OF EARTH DAMS. QUANTIFICATION OF THE DISCHARGE HYDROGRAPH

S. AMARAL(1), R. JÓNATAS(2), A. M. BENTO(3), J. PALMA(4), T. VISEU(5), R. CARDOSO(6) & RUI M. L. FERREIRA(7)

(1)(2)(4)(5)(7) *Laboratório Nacional de Engenharia Civil, Lisboa, Portugal, samaral@lnec.pt, rjljonatas@gmail.com, jpalma@lnec.pt, tviseu@lnec.pt*

(1)(3)(7) *CEHIDRO - Instituto Superior Técnico, Universidade de Lisboa, Portugal ana.bento@ist.utl.pt, ruif@civil.ist.utl.pt*

(6)(7) *ICIST - Instituto Superior Técnico, Universidade de Lisboa, Portugal rafaela@civil.ist.utl.pt*

Abstract

Dam overtopping is one of the major causes for the failure of earth dams. The objectives of the present paper are the characterization of the breach evolution and the quantification of the breach hydrograph caused by dam overtopping. To meet these objectives an embankment dam laboratory model was led to fail by overtopping under hydraulic and geotechnical controlled conditions. The data presented concerns the hydrograph, calculated by indirect and direct methods. The key features of the hydrograph are discussed attending to the observed evolution of the failure event.

Keywords: Overtopping; Dam-breach experiments; breach effluent hydrographs.

1. Introduction

Floods resulting from dam failures are responsible for devastating disasters which consequences include economical and human losses. They depend on the extension of the inundated area, the number of lives at risk and on the warning time (Wahl, 1998). Overtopping is the most common cause of failure in recent earth and earth-rockfill dams. Only embankment dams are investigated in this paper because they totalize about 3/4 of the 33 105 large dams worldwide, corresponding 88% to earth dams and 12% to rockfill dams (ICOLD, 2003).

Although there have been several small and large scale laboratory studies on earth dam failures by overtopping, that provided useful discharge hydrographs for model validation (Vaskinn et al. 2004, Zhu et al., 2011), there is still lack of phenomenological insights on the processes that occur during breach growth, which ultimately determines key features of those hydrographs.

Detailed empirical data on the breaching process are still needed, especially in what concerns the description of (i) the geotechnical discrete failure episodes during breach evolution and (ii) the interaction between hydrodynamic erosion and geotechnical failure (Wahl 2004). Such data should be gathered from laboratorial work monitored with suitable measuring methods and instrumentation, synchronized with the evolution of the failure event, and conducted under hydraulic and geotechnical controlled conditions.

This paper is aimed at characterizing the evolution of the breach resulting from dam overtopping and at quantifying the ensuing hydrograph. Two small-medium scale models of homogeneous dams were built at National Laboratory of Civil Engineering (LNEC).

The tests were conducted under hydraulic and geotechnical controlled conditions. The degree of compaction of the dams was different, as well as the shape of the pilot channels carved in the crest to localize breach formation, necessary for more accurate measurements.

Data collection included free surface variations in the reservoir, discharge in a downstream weir, breach cross-sectional area and surface velocities in the breach vicinity. Three different estimations of the breach effluent hydrograph were performed: two indirect estimations (1 - by applying the mass balance equation within the reservoir; 2 - by using the calibration curve of the downstream spillway); and one direct estimation (by associating the velocity maps of the breach surface with the breach cross section area).

2. Experimental Facilities and Instrumentation

The experimental facility at LNEC is 31.5 m long and 6.6 m wide. It allows for a maximum embankments height of 1.4 m. The embankments performed in the current work were 1.5 m wide and 0.5 m high (Figure 1).

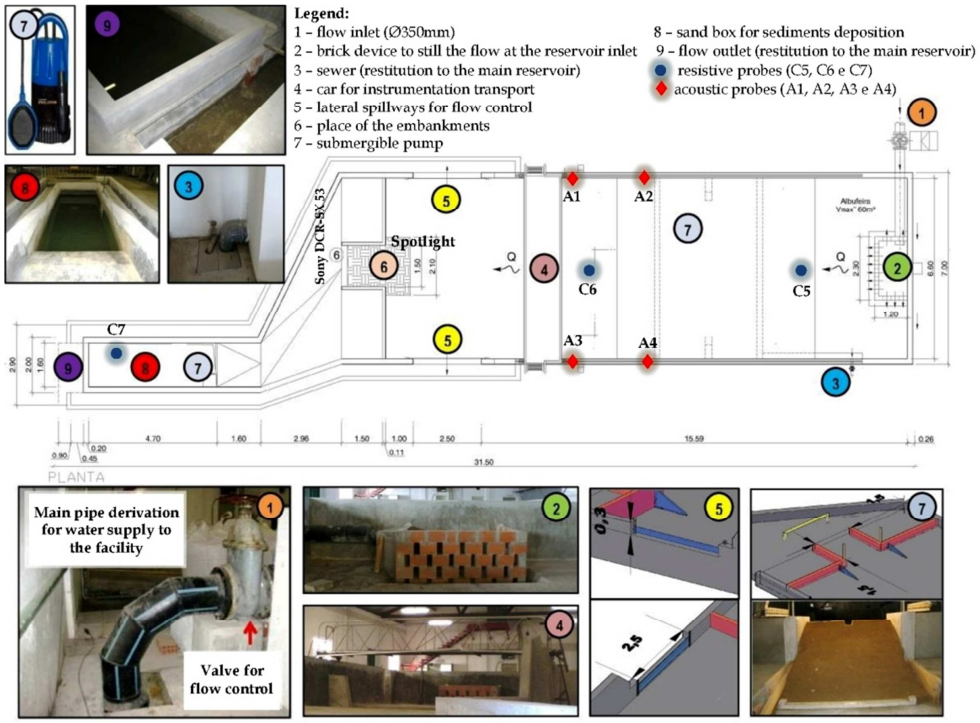

Figure 1. LNEC facility and experimental setup.

Measurements comprised i) flow discharge at the reservoir inlet, ii) temporal variation of the water elevation, within the reservoir and downstream of the dam, iii) surface flow velocity maps and iv) evolution of the breach cross-section area.

Time series of the reservoir water level were recorded by seven *water level probes*: three resistive and four acoustic probes located in strategic places (see Figures 1 and 2). A flowmeter recorded the discharge entering in the channel.

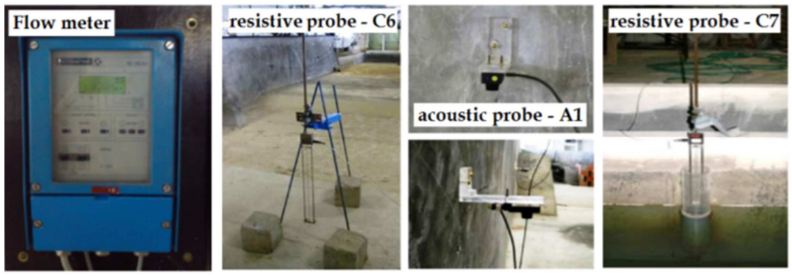

Figure 2. Instrumentation for measuring flow entering in the channel and water levels inside the reservoir.

These data allowed two indirect estimations of the breach effluent hydrographs, based on:

– the calibration curve of the downstream spillway placed at the end of the sand box;

– the mass balance of the reservoir, $dV/dt = Q_{in}(t) - Q(t)$, where V is the water volume in the reservoir, Q_{in} is the inflow discharge and Q is the breach outflow hydrograph.

The second indirect estimation had additionally the ability to consider a simple or a weighted contribution of the probes used in each test (applying Voronoï polygons within the reservoir).

Three digital video cameras were used to record the breach evolution along time. The first was positioned downstream of the embankment in order to record the frontal profile of the breach formation and evolution during overtopping phenomenon, with the aid of a 10x10 cm^2 grid drawn on the downstream face of the dam (***Erro! Auto-referência de marcador inválida.***Figure 3Figure 3). The other cameras were high-speed video cameras and were positioned above the dam crest and upstream the dam to allow, respectively, a direct quantification of surface velocities over the breach, with a LSPIV algorithm, and the estimation of the breach cross-section area (***Erro! Auto-referência de marcador inválida.***Figure 3Figure 3).

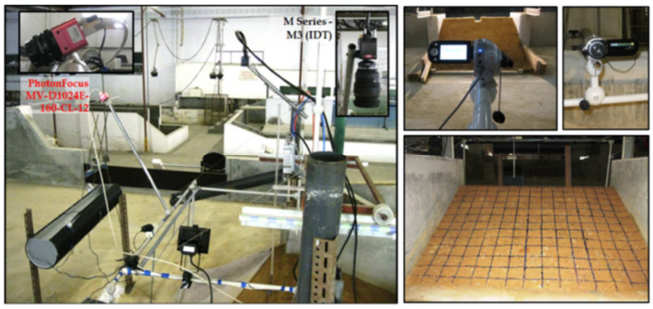

Erro! Auto-referência de marcador inválida. Figure 3. Breach evolution recording. Digital video cameras used (left photo: upstream; top right photo: downstream; bottom right photo: above the crest).

The direct estimation of the breach effluent hydrograph was obtained by combining, in each instant, the surface flow velocity maps with the breach cross-section area. The latter was obtained from the breach contour, captured by a Photonfocus high-speed camera and defined,

through digital image analysis, by the intersection of a 2W laser sheet, emitting in the green region - 532 nm (Figure 4), with the submerged part of the breach.

The velocity maps over the breach were quantified using an image-based velocity measurement algorithm (LSPIV - *Large Scale Image Particle Velocimetry*) applied to the digital images from an M3 high-speed video camera (Figure 5Figure 5). Styrofoam beads were added to the surface flow over the breach to simplify the application of the LSPIV algorithm.

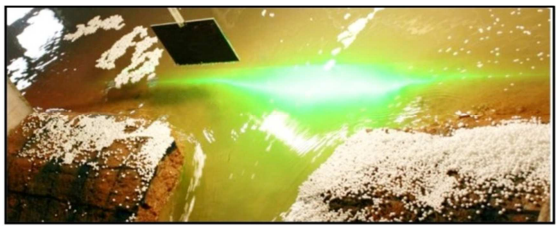

Figure 4. Laser sheet defining the breach cross-section.

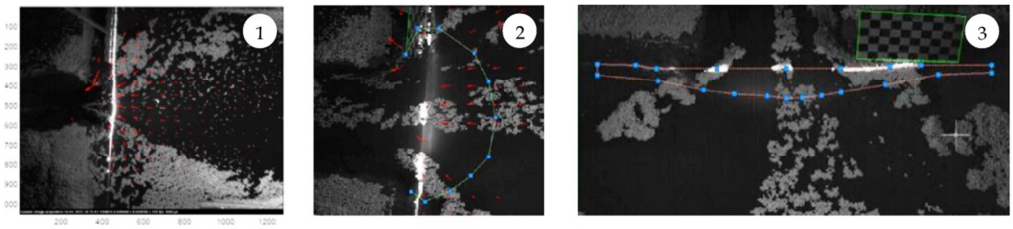

Figure 5. Example of data analysis: 1 - velocity map obtained by the application of a LSPIV algorithm; 2 and 3 – estimate of the breach cross-section area

3. Embankment Models

3.1 Soil properties and compaction procedure

Two homogeneous embankments were built for two different dam-breach experiments. Figure 6Figure 6 shows the grading size distribution curve of the soil used in both embankments (soil fractions: 6.8% of gravel, 66.0% of sand and 27.2% of fines). The specific gravity (Gs) was 2.64, liquid limit was 18% and plasticity index was 18%. The soil classifies as SM (silty sand) according to the Unified Soil Classification System. The saturated permeability measured in specimens cored from the dams after their construction was relatively low (K_{sat} = 2x10^{-8} m/s).

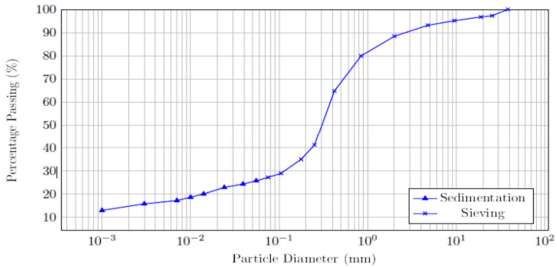

Figure 6. Grading-size distribution curve of the soil used to build the embankments.

Two Proctor compaction curves (LNEC 1966) were determined. Their optimum soil water content ($w_{optimum}$) and maximum dry volumetric weight (γ_d^{max}) are presented in Table 1.

Table 1. Proctor tests. Optimal parameters.

Curve	γ_d^{max} (kN/m³)	$w_{optimum}$ (%)
#1	20.1	9.7
#2	19.4	10.6
Average	19.8	10.2

The differences between the curves might be explained by some unavoidable soil heterogeneity. The average values of maximum dry volumetric weight and optimum water content were adopted for compaction control ($w_{optimum}$= 10.2% and γ_d^{max}= 19.8 kN/m³).

Two trial embankments were built before the construction of the dams in order to ensure a proper compaction. Further details are given in Bento (2013). The embankments of each dam-breach experiment were performed using the compaction method of the first trial embankment, (with a wood rod sheaf coupled to a wood plate at the bottom with a 0.10 m layer thickness) although applying different compaction energies.

3.2 First embankment

The embankment built for the first experiment had height of 0.48 m and crest width of 0.17 m, as shown in Figure 7. The crest length of the embankment was 1.00 m. The upstream slope was 1V:3H while the downstream slope was 1V:2.5H. Both angles are smaller than the shear strength angle φ′ expected for this type of materials.

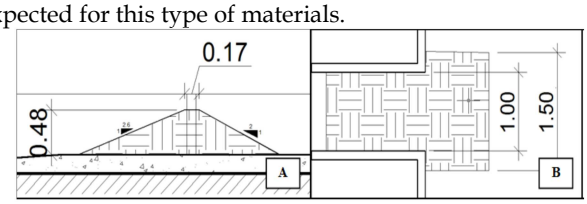

Figure 7. Geometry of the first embankment.

Compaction was done adopting a multiple layer system (0.10 m thick) to ensure homogeneity in soil properties. Relatively low compaction energy was applied (four blows per location in each layer) in the first trial embankment to speed up construction.

The embankment was shaped with the aid of a set-square as a trowel. An initial rectangular shaped breach section with 0.10x0.055 m² (width x height) was carved in the center of the embankment crest (Figure 8Figure 8) to control the area of concentrated flow and the initial erosion at the beginning of the overtopping phenomenon, and also to mitigate the effects of the facility side walls.

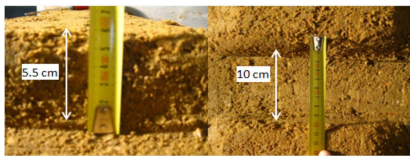

Figure 8. Rectangular pilot channel.

3.3 Second embankment

The length of the embankment crest for the second experiment was 0.15 m. This embankment had a height of 0.45 m, a crest width of 0.17 m, and, slope of 1V:2H at upstream and at downstream (Figure 9). As for the first embankment, both slope angles were smaller than φ'.

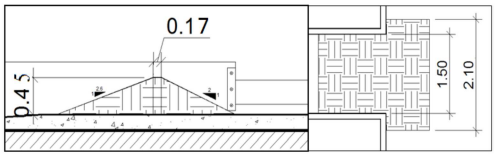

Figure 9. Geometry of the second embankment.

This embankment was built as the first, but twelve blows were applied instead of four, in order to reach the minimum degree of compaction of 85% defined using the Proctor parameters already presented. Compaction interval was (γ_d^{max}= 19.8 kN/m³) and a water content within the interval w ∈ [$w_{optimum}$; $w_{optimum}$ + 2%]. Four samples were extracted during the construction for compaction control. Upstream slope was compacted confined by a wood triangular framework (0.45 m length and 0.90 m high), mounted in each lateral side of the embankment. Shaping was done using a set-square as a trowel, as for the first embankment. The carved pilot channel was carved with triangular shape with 1V:1H side slopes and 0.02 m depth at the center of the crest. Both geometry and photograph of the downstream view of the pilot channel are presented in Figure 10 and 11, respectively.

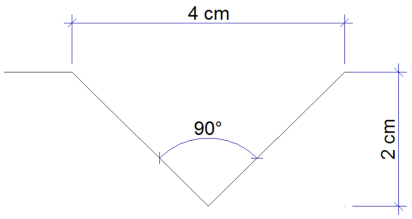

Figure 10. Geometry of the pilot channel.


Figure 11. Triangular pilot channel.

4. Results

Summary of experiments

Two different dam-breach experiments were performed, for the dams previously described. The indirect estimations of the breach outflow hydrographs were obtained in both experiments but the direct estimation was only attained in the second.

Table 2Table 2 resumes the main characteristics of each experiment.

Table 2. Main characteristics of embankments.

Experiments	Embankment			Upstream slope	Downstream slope	Compaction layers thickness (m) / nº of blows/ % of compaction	Pilot Channel			Breach hydrographs estimations
	height (m)	crest width (m)	crest length (m)				Shape	Dimensions		
1	0.48	0.17	1.00	1V:3H	1V:2.5H	0.10 / 4 blows / 82%	rectangular	0.10 m wide	0.055 m high	2 indirect estimations
2	0.45	0.17	1.50	1V:2.0H	1V:2.5H	0.10 / 12 blows / 90%	triangular	1V:1H side slopes	0.020 m depth	2 indirect estimations 1 direct estimation

4.1.1 First experiment

The breach outflow hydrograph in the first experiment was predicted by two indirect estimates, presented in Figure 12Figure 12, namely from the spillway calibration curve (blue line in Figure 12) and the mass balance of the reservoir (black line in Figure 12). The spillway estimate is unreliable for discharges higher than the upper range of calibration (details in Bento, 2013, Jónatas, 2013).

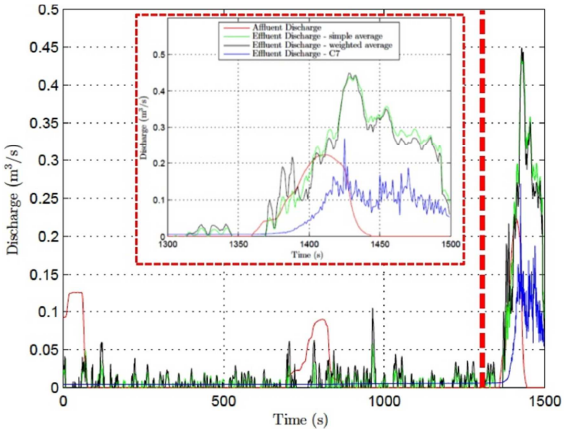

Figure 12. First experiment. Indirect estimates of the breach outflow hydrograph

In Figure 13 it can be seen that:

1. in the initial stage of the dam failure (t < 1380 s):

1.1 the breach outflow hydrograph estimated from the spillway provides a good estimate since the flow velocity inside the sand box is still relatively low and the effluent discharge is within the range of the spillway discharge rating curve (without extrapolation);

1.2 the breach outflow hydrograph obtained using balance of water mass within the reservoir (black and green lines in Figure 12Figure 12) is not reliable since the noise amplitude of the estimate is higher than the estimated flow values;

2. from the moment the overtopping phenomenon becomes more pronounced (t > 1380 s):

2.1 the high agitation inside the sand box did not allowed reliable data levels acquisition; additionally, the water heights above the spillway crest were out of the range of the spillway rating curve and therefore, the spillway estimate was no longer reliable;

2.2 although there is still noise present in the breach outflow estimate, its amplitude is approximately constant and much lower than the estimated flow values; therefore, at this stage, this is the reliable estimate;

3. the inertia of the flow inside the facility cannot be neglected, as it can be verified by the approximately 15 seconds lag between the increase of the affluent and the effluent discharge;

4. a quite similar behavior of the breach hydrographs estimated using balance of water mass within the reservoir was observed using an equal or a weighted contribution of all the probes used in the data acquisition of the water levels inside the reservoir;

5. a peak outflow discharge of approximately 450 l/s was observed.

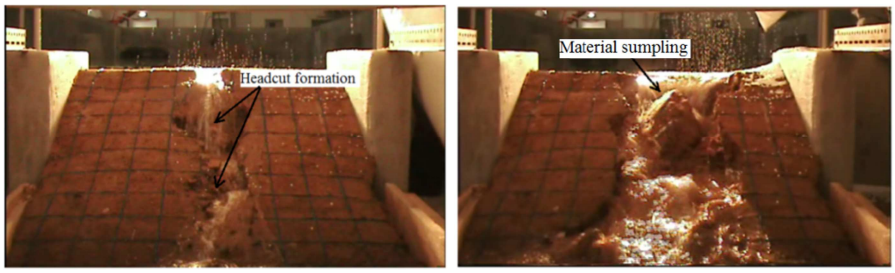

Figure 13. First experiment. Examples of undercutting and material slumping.

The erosion process in this first experiment was mainly of hydraulic nature, although it was also observed failure by undercutting (Figure 13Figure 13). This phenomenon induced falling of soil blocks caused by loose of their base, causing first a dumping failure and then the entire embankment failure.

4.1.2 Second experiment

The breach outflow hydrograph in the second experiment was predicted by two indirect and by one indirect estimates, presented in Figures 14 and 15 respectively.

In Figure 14Figure 14 it can be seen that:

1. $Q_{Effluent} < 100$ l/s $\rightarrow$ the breach outflow hydrograph obtained with the spillway calibration curve is the best estimate;
   $Q_{Effluent} > 120$ l/s $\rightarrow$ the breach outflow hydrograph obtained using the balance of water mass within the reservoir is the best estimate;
   00 l/s < $Q_{Effluent}$ <120 l/s $\rightarrow$ both estimates are valid and practically coincident;
2. around t = 3000 s a significant increase of the effluent discharge (~ 40 l/s) occurs and is accompanied by a much smaller increase of the affluent discharge, without difference in the reservoir level (explained by a sudden detachment of dam material which resulted in an increase of the breach cross-section area);

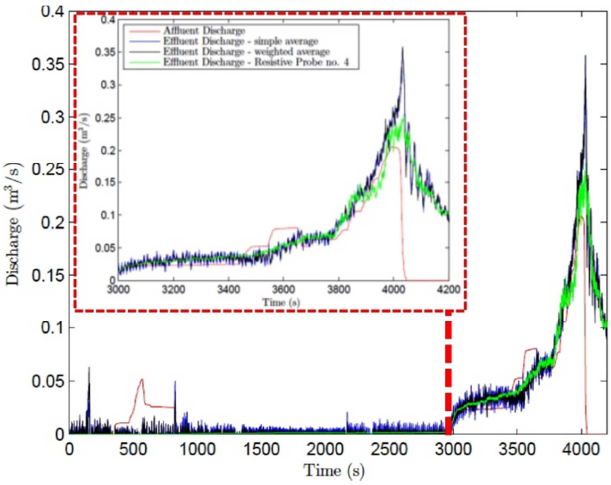

Figure 14. Second experiment. Indirect estimates of the breach outflow hydrograph.

3. the inertia of the flow inside the facility cannot be neglect in this second experiment neither; however the temporal lag between the increase of the affluent and the effluent hydrographs is less evident in this second experiment than in the first one, mainly because of the failure phenomenon, which was about ten times slower in this last experiment;
4. similar behavior of the breach hydrographs estimated using the balance of water mass within the reservoir was observed using an equal or a weighted contribution of all the probes used in the data acquisition of the water levels inside the reservoir;
5. a peak outflow discharge of approximately 360 l/s was observed.

Figure 15 shows that there is a good agreement between direct and indirect estimates in the domain where it was possible to determine the former.

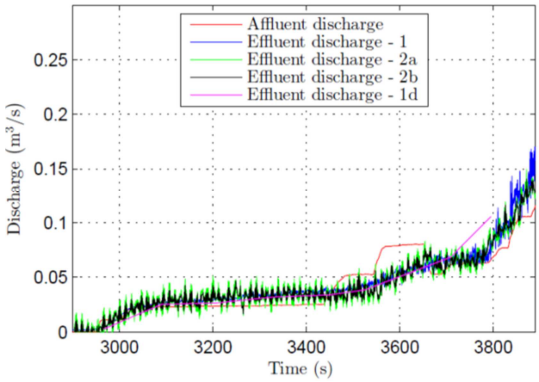

Figure 15. Second experiment. Comparison between the indirect and direct estimates of the breach outflow hydrograph

The direct estimation of the breach effluent discharge was not possible to perform until the instant of the peak discharge mainly due to: 1) the lack of sufficient styrofoam beads in the flow to allow the determination of the velocity with the LSPIV algorithm; and 2) the difficulty to accurately define the upstream parabolic shape of the breach (Figure 12).

As observed in the first experiment, the erosion process in this second experiment was also of hydraulic nature, with some episodes of undercutting (Figure 16).

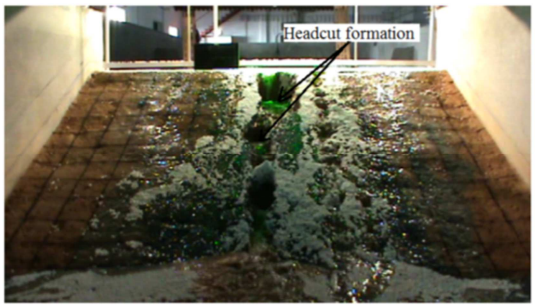

Figure 16. Second experiment. Example of undercutting.

5. Conclusions

This paper presents the estimates of the discharge hydrographs resultant form the failure by overtopping of two earth dams where two parameters were varied: 1) the degree of compaction of the embankment, and 2) the geometry of the pilot channel.

The two experiments performed allowed the following general conclusions:

- reliable estimates of the breach discharge hydrograph can be achieved by combining both indirect estimates: the calibration curve of the downstream spillway, for the low discharges, and the balance of water mass in the reservoir for the higher discharge values;
- higher degrees of compaction influence the breach development in what concerns the breaching time and the reservoir volume discharged between initiation and peak instants;
- the geometry of the *pilot channel* did not seem to influence the breach final form, however, these two experiments were not sufficient to understand the entire influence of these two parameters on the breach morphological evolution;
- although the breaching process of both experiments was mainly due to hydraulic erosion, it was also observed erosion by undercutting which contradicts the failure predominately by regressive erosion that has been widely referred in the literature.

These two experiments contributed for a better understanding of the influence of the embankment compaction degree in the breaching process. However, to deepen this knowledge and conclude about the influence of these two parameters, a set of experiments with different compaction energies and pilot channels geometries should be performed in the future.

Beyond these parameters, others should be studied trippingly in order to perceive their importance in the erosive process of the dam, such as the grain-size distribution curves, the upstream and downstream slopes and the type of earth dam (homogeneous versus zoned).

Acknowledgments

The authors thank the following groups of LNEC: the *Laboratorial Construction and Modeling Team* for support in developing solutions to improve the experimental setup; the *Geotechnical Department* (DG) throughout the entire geotechnical analysis; and the *Centre of* Scientific Instrumentation (CIC) for support in the instrumentation phase of the tests.

The work was partially funded by the Portuguese Foundation for Science and Technology (FCT) through project RECI/ECM-HID/0371/2012. First author thanks FCT for financial support through PhD scholarship SFRH/BD/47694/2008.

References

Bento, A. M. (2013). Characterization of dam breaching following overtopping, Master's thesis, Instituto Superior Técnico. Universidade Técnica de Lisboa

Especificação, L. (1966). E197, solos. Ensaio de compactação, LNEC, Lisboa.

ICOLD (2003). 21ºICOLD Congress, Montreal.

Jónatas, R. (2013). Rotura de barragens de aterro por galgamento. Ensaios experimentais com aterros homogéneos. Master's thesis, Faculdade de Ciências, Universidade de Lisboa

Vaskinn, K. A., Løvoll, A., Höeg, K. (2004). Breach formation - Large scale embankment failure. Detailed Technical Reports of Impact Project - NAS Norway.

Wahl, T. (2004). Uncertainty of predictions of embankment dam breach parameters. Journal of hydraulic engineering 130(5), 389_397.

Wahl, Tony L. (1998). Preditions of Embakment Dam Breach Parameters. Dam Safety Research Report , Julho de 1998: 7-10.

Zhu, Y., Visser, P., Vrijling, J. & Wang, G. (2011). Experimental investigation on breaching of embankments. Science China Technological Sciences 54(1), 148_155.